

An Experimental Study on the Thermal Performance of a Concentric Annular Heat Pipe

Joon Hong Boo*, Soo Yong Park

*School of Aerospace and Mechanical Engineering, Hankuk Aviation University,
200-1, Hwajeon-dong, Deogyang-gu, Goyang-city, Gyeonggi-do 412-791, Korea*

Do Hyoung Kim

EWIC Co., Ltd.,

7-1, Majang-ri, Gwangtan-myun, Paju-city, Gyeonggi-do 413-851, Korea

Concentric annular heat pipes (CAHP) were fabricated and tested to investigate their thermal characteristics. The CAHPs were 25.4 mm in outer diameter and 200 mm in length. The inner surface of the heat pipes was covered with screen mesh wicks and they were connected by four bridge wicks to provide liquid return path. Three different heat pipes were fabricated to observe the effect of change in diameter ratios between 2.31 and 4.23 while using the same outer tube dimensions. The major concern of this study was the transient response as well as isothermal characteristics of the heat pipe outer surface, considering the application as uniform heating device. A better performance was achieved as the diameter ratio increased. For the thermal load of 180 W, the maximum temperature difference on the outer surface in the axial direction of CAHP was 2.3°C while that of the copper block of the same outer dimension was 5.9°C. The minimum thermal resistance of the CAHP was measured to be 0.04°C/W. In regard to the transient response during start-up, the heat pipe showed almost no time lag to the heat source, while the copper block of the same outer dimensions exhibited about 25 min time lag.

Key Words: Concentric Annular Heat Pipe, Diameter Ratio, Fill Charge Ratio, Start-Up Characteristics, Isothermal Characteristics

Nomenclature

h_{max} : Gap between the inner and outer pipes (m)
 K : Wick permeability (m²)
 L_{eff} : Effective heat pipe length (m)
 Δp_f : Pressure drop due to liquid friction (Pa)
 Q_{input} : Input thermal load (W)
 R_d : Diameter ratio : outer diameter of outer pipe / inner diameter of inner pipe
 R_{HP} : Thermal resistance of heat pipe (°C/W)

r_c : Capillary radius (m)
 \bar{T}_{evp} : Average temperature of evaporator (°C)
 \bar{T}_{con} : Average temperature of condenser (°C)
 \bar{v}_l : Apparent liquid velocity through porous medium (m/s)

Greek symbols

μ_l : Liquid viscosity (N·s/m²)
 ρ_l : Liquid density (kg/m³)
 σ : Surface tension of liquid (N/m)
 ϕ : Fill charge ratio of working fluid (%):
 (charged liquid volume / total wick pore volume) × 100

* Corresponding Author,

E-mail : jhboo@hau.ac.kr

TEL : +82-2-300-0107; FAX : +82-2-3158-2191

School of Aerospace and Mechanical Engineering,
 Hankuk Aviation University, 200-1, Hwajeon-dong,
 Deogyang-gu, Goyang-city, Gyeonggi-do 412-791,
 Korea. (Manuscript Received November 5, 2004; Re-
 vised February 25, 2005)

1. Introduction

A cylindrical heat pipe has an evaporator and a condenser in the axial direction of the pipe and

thermal energy is transferred along the axial direction. In a concentric annular heat pipe (hereinafter denoted by CAHP), however, the evaporator and the condenser is separated in the radial direction and thermal energy is transferred in the radial direction. It is sometimes called as a 'coaxial heat pipe'. Fig. 1 compares the operating principles of the conventional heat pipe and the concentric annular heat pipe (Peterson, 1994). The CAHP in this study is composed of two concentric pipes of unequal diameters, a screen mesh wick, and four bridge wicks. A heat source is inserted in the inner pipe which functions as the evaporator region. The CAHP of this type can be applied to the heating of drum or roll in the laser printers or copy machines where an isothermal heating as well as rapid response is desired (Park and Boo, 2004).

The concept of the CAHP was introduced by Vasiliev (1973) named it as co-axial heat pipe. He evaluated the performance of the heat pipe by the input thermal loads and the temperature of the radial direction. Faghri and Thomas (1989) proposed new concentric annular heat pipe design to increase the heat transport capacity having same external shape. It consisted of two concentric pipes of unequal diameters attached by means of end caps. The heat pipe had two evaporators and two condensers at the outer and inner surface and the design brought the increase of the heat transfer area. They compared the result with the performance of the conventional heat pipe with same outer dimensions and verified improvement of the thermal performance. Recently, Kim et al. (2003) conducted the start-up test of heat pipe type heating roller which can substitute the halogen lamp in a laser printer. The evaporator of the heat pipe was whole surface of the container and the temperature transient was observed.

Although the concept and operating principle are readily available through existing literature, and few analytical studies of the CAHP have been conducted thus far, quantitative investigation based on experimental studies has yet to be provided, including the effects of important design parameters such as diameter ratio and fill charge ratio of working fluid. The purpose of this

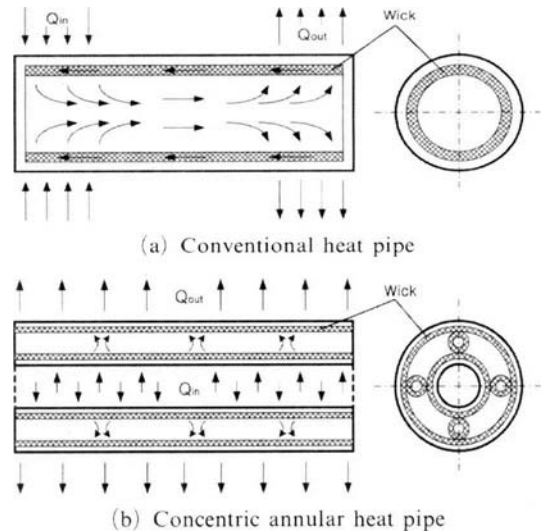


Fig. 1 Schematic of the concentric heat pipe as compared with the conventional one

study is to investigate experimentally the thermal performance of CAHP with different diameter ratios and fill charge ratios for both steady-state and start-up operation. Three different ratios of inner diameter to outer diameter of the CAHP were compared and a copper block with same shape was tested to compare the start-up performance. Furthermore, fill charge ratio which renders the optimum performance was identified and discussed.

2. Experimental Setup and Procedures

The major objective of this study is to estimate the effect of diameter ratio change on the performance of CAHP. The outer diameter of outer pipe was 25.4 mm and the inner diameters of the inner pipes were 11 mm, 8 mm, and 6 mm, respectively, as shown in Fig. 2. These values corresponded to the diameter ratios (R_d) 2.31, 3.18, and 4.23, respectively. All the pipes were 200 mm in length and the both sides were closed by end caps. Fig. 2 shows the cross sections of the CAHP fabricated for this study.

The container material was copper and the screen wick was made of stainless steel. As circumferential wicks to distribute liquids evenly

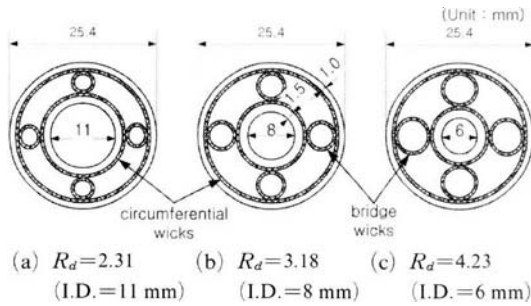


Fig. 2 Cross sections of CAHP

over the evaporator and condenser surfaces, double layers of 80 mesh screen wick were attached to the inner surfaces of the heat pipe walls. To provide liquid return paths in CAHP, the bridge wicks were inserted between the circumferential wicks in the evaporator and condenser surfaces. While many options were available for shape and size of the bridge wicks, a wrapped-screen type was selected in this study for easiness in fabrication. Four bridge wicks made of double layers 80-mesh screen were used in each CAHP. The pore size of wick was determined considering the liquid friction pressure drop and pressure head of working fluid from the following equation.

$$\frac{2\sigma}{r_c} \geq \Delta p_f + \rho_l g h_{\max} \quad (1)$$

$$= \left(\frac{\mu_l \bar{v}_l L_{eff}}{K} \right) + \rho_l g h_{\max}$$

where σ is the surface tension of working fluid, r_c is the capillary radius of the wick, Δp_f is the pressure drop due to liquid friction, μ_l is the liquid viscosity, \bar{v}_l is the apparent liquid velocity through wick, K is the permeability, L_{eff} is the effective heat pipe length, and h_{\max} is maximum rising height of working fluid, which corresponds to the gap between the inner and outer pipes. The largest h_{\max} value for the bridge wick in this study was 7.2 mm for CAHP as shown in Fig. 2(c).

The working fluid was distilled water. Filling quantities were calculated based on the volume of the wick pore. The total pore volumes of three CAHPs (a), (b), and (c) in Fig. 2 were 10.1 cc, 10.9 cc, and 11.1 cc, respectively, which corresponded to 100% fill charge amount in each CAHP. The fill charge ratio, ϕ , in this study was

Table 1 Specification of the CAHP

R_d (O.D./I.D.)	2.31	3.18	4.23
O.D. (mm)	25.4		
Wall Thickness of Outer Pipe (mm)	1.0		
I.D. (mm)	11	8	6
Wall Thickness of Inner Pipe (mm)	1.5		
Container Material	Copper		
Wick Material	Stainless Steel		
Screen Mesh Number	80		
Total Pore Volume (cc)	10.1	10.9	11.1

defined as follows.

$$\phi(\%) = \frac{\text{charged liquid volume}}{\text{total wick pore volume}} \times 100 \quad (2)$$

Fill charge ratios varied from 20% to 100%. Table 1 summarizes the specifications of the fabricated CAHP in this study.

A cartridge type electric heater was inserted in the inner pipe as a heat source. The outer diameter of heater was made equal to the inner diameters of three CAHPs. Since the container of the heater was made of stainless steel and non-homogeneous array of the coiled wire was fixed by magnesium powder, the heat flux on the surface was essentially non-uniform. The total thermal load was controlled by variable AC transformer and monitored by a wattmeter.

The wall temperatures were measured by K-type thermocouples. Fifteen thermocouples were mounted on the outside surface and four thermocouples were inserted and attached to the inner wall. The length from the end of the inserted thermocouples to the end cap was 60 mm. Fig. 3 shows the location of mounted thermocouples. Five thermocouples located on the top of the CAHP in axial direction. In circumferential direction, seven thermocouples were attached at the center axial location of the CAHP.

Figure 4 shows the schematic of the experimental setup. Two small fans were used to cool the heat pipe by forced convection. To concentrate cooling air, a tapered duct of 400(L)mm

was used and the distance from duct to CAHP was about 50 mm. The dimensions of duct inlet and outlet were 250(W) × 125(H) and 250(W) × 30(H) mm, respectively, and the mean velocity of the outlet was measured about 3 to 4 m/s.

To investigate the start-up performance, the temperature variation of the copper block and the CAHP with $R_d=2.31$ were observed and compared. Moreover, the axial temperature differences on the heat pipe surface were measured as functions of the diameter ratio and the fill charge ratio. Fill charge ratio of each heat pipe was changed and the optimum ratio was discussed. The thermal resistances of the CAHP were calculated, using the following equation.

$$R_{HP} = \frac{\bar{T}_{evp} - \bar{T}_{con}}{Q_{input}} \quad (3)$$

where \bar{T}_{evp} is the average temperature of the evaporator surface, \bar{T}_{con} is the average temperature of the condenser surface, and Q_{input} is the input thermal load.

Considering the properties of water as working fluid and the safety of CAHP, the operating temperature limit of 200°C was imposed throughout the experiment in this study as recommend-

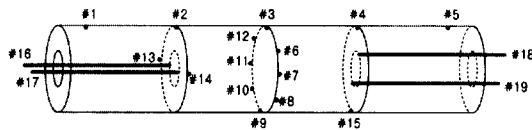


Fig. 3 Thermocouples locations

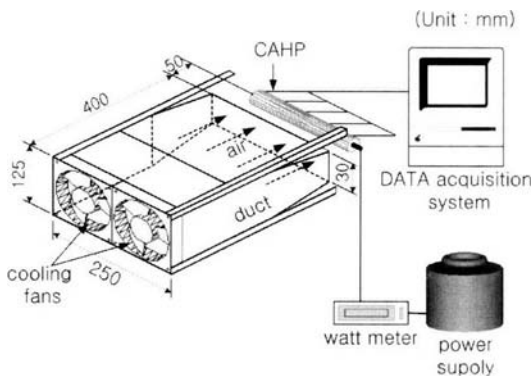


Fig. 4 Experimental setup

ed by literature (Peterson, 1994). The maximum thermal load value appeared in each case of experiment corresponded to this temperature limit and it was not associated with the conventional operating limit of heat pipes (e.g. capillary limit).

3. Results and Discussion

3.1 Start-up characteristics

Figure 5 compares the start-up characteristics of the copper block and the CAHP ($R_d=2.31$, I.D.=11 mm) with same outer size and shape against the cartridge heater, which was a heat source, for input thermal load of 120 W. The cartridge heater had outer diameter of 11 mm and the surface area of 69 cm². The outer surface areas of the copper block and the CAHP were the same with 160 cm², which was 2.3 times of the heater surface. The temperature difference between the heater and the others was resulted from the thermal resistance between the heat source and the outer surface of the CAHP or copper block and the heat transfer area at the same input thermal load. For the heater, the transient time before the steady state was 25 minutes, approximately. The transient time for the CAHP was almost same as the cartridge heater. The copper block required over 50 minutes to reach a steady state. The result proved that the CAHP exhibited fast thermal response typical for heat pipes in normal operation.

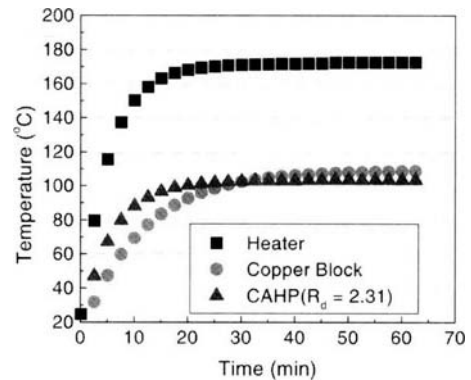
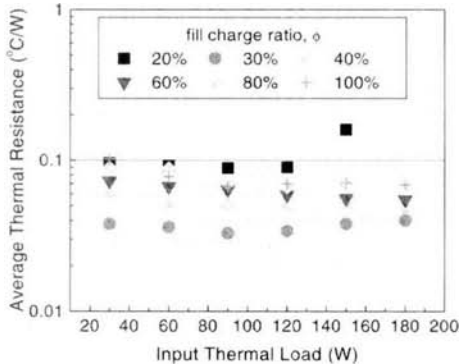


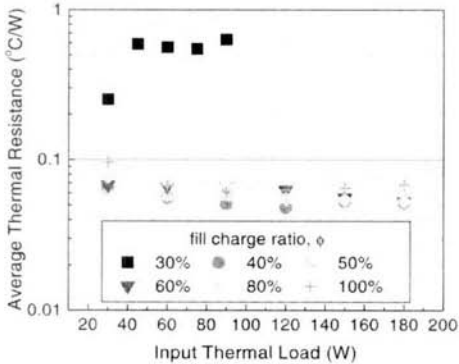
Fig. 5 Transient temperature responses for input thermal load of 120 W

3.2 Thermal resistance

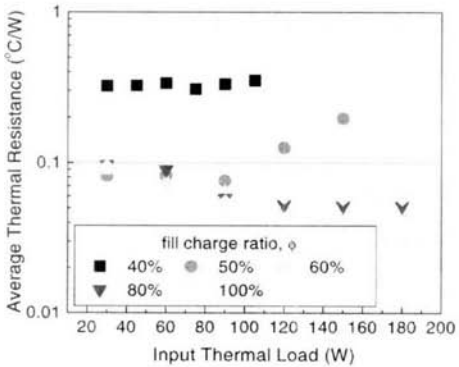
Figure 6 shows the average thermal resistances of the CAHP as a function of fill charge ratio for each diameter ratio. It is clear from Fig. 6(a) that for the CAHP with $R_d=2.31$, the optimum fill charge ratio for the lowest thermal resistance was



(a) $R_d=2.31$ (I.D.=11 mm)



(b) $R_d=3.18$ (I.D. = 8 mm)



(c) $R_d=4.23$ (I.D. = 6 mm)

Fig. 6 Average thermal resistances of CAHP as functions of input thermal load and fill charge ratio

30%. For $\phi=100%$, the thermal resistance ranged from 0.07 to 0.1°C/W. The increase of the thermal load slowly reduced the thermal resistance for $\phi=40%$ or higher. For $\phi=40%$, the decrease of the thermal resistance was observed from 0.05 to 0.06°C/W when thermal load increased from 30 W to 180 W. For $\phi=20%$, thermal resistance increased rapidly at 150 W thermal load due to sudden increase of evaporator temperature near dry-out.

The thermal resistance of the CAHP with $R_d=3.18$ is shown in Fig. 6(b) as a function of the fill charge ratio and the input thermal loads. Except those for $\phi=30%$, the resistances ranged from 0.05 to 0.1°C/W. The least value occurred for $\phi=40%$. For $\phi=30%$, the values were extremely higher due to a dry-out near thermal load 120 W.

Figure 6(c) shows the variation of the thermal resistance of the CAHP with $R_d=4.23$. The increase of the thermal load resulted in the decrease of the thermal resistance for $\phi=60%$ or higher. The optimum fill charge ratio was 60% for the least thermal resistance which ranged from 0.05 to 0.09°C/W. For $\phi=50%$, thermal resistance exhibited increase for input thermal load higher than 90 W due to a near-dry-out trend. For $\phi=40%$, the values were much higher than others and a dry-out occurred at 120 W.

The comparison of the optimum thermal resistance was shown in Fig. 7. The compared fill charge ratios were 30%, 40%, and 60%, respec-

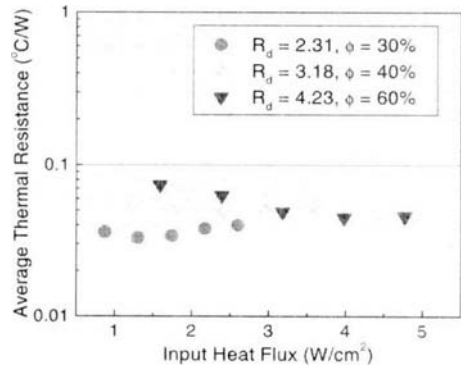


Fig. 7 Average thermal resistances for optimum fill charge ratio

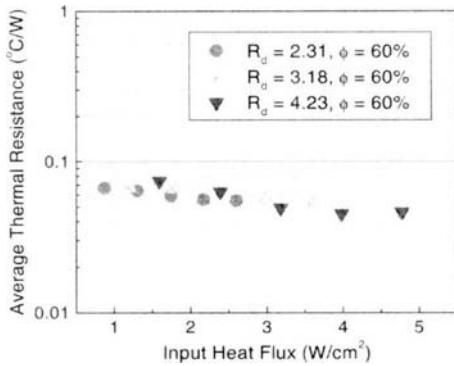


Fig. 8 Average thermal resistances for 60% fill charge ratio

tively. The thermal input loads were converted to the heat flux. The thermal resistances of the CAHP were measured from 0.036 to 0.074°C/W depending on the diameter ratio and input heat flux. The CAHP with $R_d=2.31$ exhibited the least thermal resistance for the same input heat flux.

Figure 8 shows the variation of the thermal resistance of all CAHPs in this study with $\phi=60\%$. The thermal resistance values ranged from 0.046 to 0.067°C/W and the change of the inner diameter did not result in a noticeable deviation. Fig. 7 showed rather scattered data among the CAHP than those in Fig. 8. The change of fill charge ratio was more influential than the variation of the diameter ratio.

3.3 Maximum temperature difference

The CAHP was cooled by forced convection using fan and duct in this study considering its applications. Under forced convection as depicted in Fig. 4, a considerable temperature differences would be resulted from different cooling conditions along the circumferential direction of CAHP. Therefore, the circumferential temperature distribution may not represent the thermal characteristics of CAHP. To investigate the isothermal characteristics of a CAHP, it was thought reasonable to observe the temperature along the axial locations having the same cooling condition. To estimate the effect of natural convection however, temperatures were measured at eight points along the circumference of the CAHP at

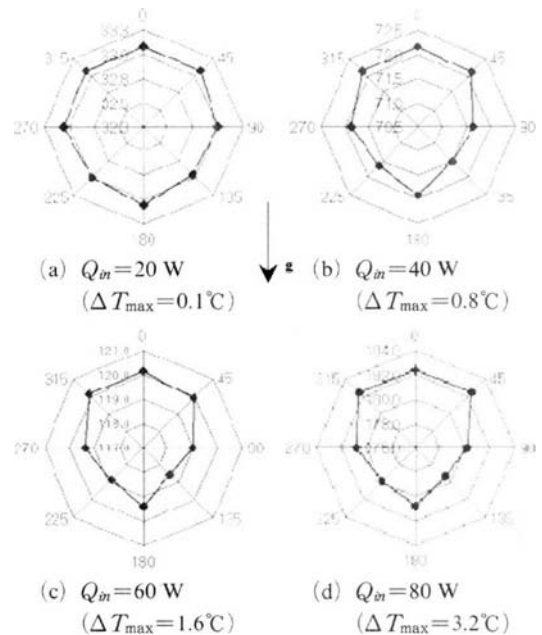


Fig. 9 Temperature distribution in circumferential direction of CAHP under natural convection cooling (measured at the center axial location)

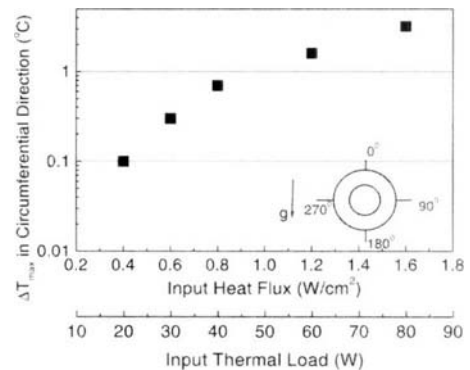


Fig. 10 Maximum temperature difference in the circumferential direction of a CAHP with $R_d=2.31$ and $\phi=100\%$ under natural convection cooling (measured at the center axial location)

the center axial location as depicted in Fig. 3.

Figures 9 and 10 summarize the circumferential temperature distribution of a CAHP with $R_d=2.31$ and $\phi=100\%$ under natural convection cooling. The maximum temperature occurred always at the top position (where $\theta=0^\circ$) due to

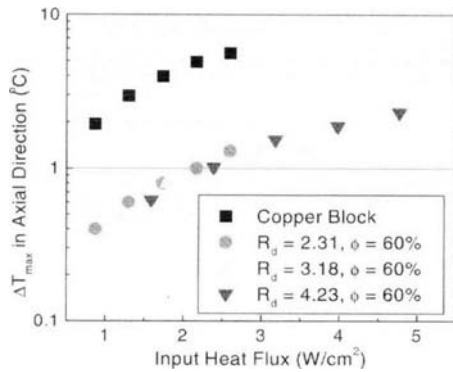


Fig. 11 Maximum temperature difference in axial direction of CAHP with 60% fill charge ratio under forced convection cooling

the influence of buoyancy. The temperature distribution appeared to be symmetrical in the horizontal direction (See Fig. 9). The maximum temperature difference was only 0.1°C when input thermal load was 20 W, but the same was 3.2°C when the input thermal load was 80 W (See Fig. 10). Temperature data for thermal loads higher than 80 W (heat flux: 1.6 W/cm²) with natural convection cooling were not obtained since the CAHP temperature exceeded 200°C, which is normally the operating temperature limit for water heat pipes. For the same CAHP ($R_d=2.31$, $\phi=100\%$) was under forced convection cooling, the maximum input thermal load was 180 W (heat flux: 3.6 W/cm²) while keeping the maximum operating temperature below 200°C.

In Fig. 11 the maximum axial differences of the CAHPs with $\phi=60\%$ are shown and compared with those of the copper block. The axial temperature difference of the copper block ranged from 2.0 to 5.9°C. For the same input heat flux range, those for $R_d=2.31$ ranged from 0.4 to 1.3°C. As a result, the axial temperature difference of the copper block showed maximum of five times larger value than those for $R_d=2.31$. The CAHP with $R_d=4.23$ exhibited the largest input heat flux and the difference increased from 0.6 to 2.3°C.

For the same range of heat flux, the diameter ratio did not result in a notable difference in the thermal resistance. The increase of the heat flux caused a logarithmic increase of the axial temperature difference.

4. Conclusions

Based on a series of experiments performed in this study, the following conclusions can be stated for CAHPs having diameter ratios between 2.3 and 4.2 (for the same outer diameter of 25.4 mm), fill charge ratios between 20% and 100%, and input heat flux up to 4.77 W/cm² (thermal load 180 W).

(1) During the start-up transient, no time lag in the temperature response was observed between the heat source and the CAHP. In the copper block, however, about 25 minutes of time lag was observed.

(2) For the same fill charge ratio of the CAHP, the diameter ratio had only little influence on the thermal resistance. However, the fill charge ratio significantly affected the thermal resistance of the CAHP as the diameter ratio increased.

(3) The isothermal characteristics of CAHP were excellent. At the heat flux of 2.6 W/cm², for example, the axial temperature difference was only about 1°C compared with about 6°C for a copper block of the same outer dimension.

(4) Therefore, the CAHP similar to those in this study can be utilized effectively in many applications where an isothermal as well as fast-response heating device is desired.

References

- Faghri, A. and Thomas, S., 1989, "Performance Characteristics of a Concentric Annular Heat Pipe: Part I-Experimental Prediction and Analysis of the Capillary Limit," *Journal of Heat Transfer*, Vol. 111, No. 4, pp. 844~850.
- Kim, K. S., Kim H. B. and Lee, K. W., 2003, "Development of Heat Pipe Heating Roller in Laser Printer," *Proceedings of The 7th International Heat Pipe Symposium*, Jeju, Korea, pp. 65~69.
- Kim, D. H., Park, S. Y. and Boo, J. H., 2004, "A Study on the Thermal Performance of Concentric Annular Heat Pipes," *Proceedings of the KSME Spring Annual Meeting in Korea*,

pp. 1412~1417.

Peterson, G. P., 1994, *An Introduction to Heat Pipes : Modeling, Testing, and Applications*, John Wiley & Sons, Inc., pp. 1~7.

Vasiliev, L. L., 1973, "Heat and Mass Transfer in Low Temperature Heat Pipes," *Proceedings of The 1st International Heat Pipe Conference*, Stuttgart, Germany, 3-1.